Forestry An International Journal of Forest Research

Institute of Chartered Foresters

Forestry 2013; **86**, 463–473, doi:10.1093/forestry/cpt017
Advance Access publication 3 July 2013

Assessment of Cartosat-1 and WorldView-2 stereo imagery in combination with a LiDAR-DTM for timber volume estimation in a highly structured forest in Germany

Christoph Straub[1]*, Jiaojiao Tian[2], Rudolf Seitz[1] and Peter Reinartz[2]

[1]*Department of Information Technology, Research Group: Remote Sensing, Bavarian State Institute of Forestry (LWF), Hans-Carl-von-Carlowitz-Platz 1, D-85354 Freising, Germany*
[2]*Earth Observation Center, Remote Sensing Technology Institute, Photogrammetry and Image Analysis, German Aerospace Center (DLR), Oberpfaffenhofen, 82234 Wessling, Germany*

*Corresponding author. E-mail: christoph.straub@lwf.bayern.de

Received 8 November 2012

Stereo satellites provide height information of the earth's surface with increasing accuracy. High temporal resolution and wide regional coverage are the great advantages of satellites compared with aerial surveys. There is currently little experience of how accurate forest attributes can be modelled using high-resolution stereo satellite data, especially for highly structured forests in Central Europe. Thus, the potential of Cartosat-1 and WorldView-2 was assessed for timber volume estimation in a complex forest in Germany. Digital surface models were generated using Semi-Global Matching. Canopy height models (CHMs) were computed by subtracting a Light detection and ranging (LiDAR) terrain model. The CHMs were co-registered with field plots of a forest inventory. Explanatory variables were derived from the CHMs for timber volume estimation using regressions. Accuracies were evaluated at plot and stand levels. Results were compared with estimations based on a LiDAR-CHM. At plot level the following root mean squared errors (RMSEs) for timber volume estimation were obtained: 50.26 per cent for Cartosat-1, 44.40 per cent for WorldView-2 and 38.02 per cent for LiDAR. The RMSEs were smaller than the standard deviation of the observed timber volume. The RMSEs at a stand level yielded 21.49 per cent for Cartosat-1, 19.59 per cent for WorldView-2 and 17.14 per cent for LiDAR. The study demonstrates the potential of satellite stereo images for regionalization of sample plot inventories.

Introduction

Cost-efficient monitoring systems are required to accomplish the increasing demand for accurate information about the status and the production potential of forests. In general, terrestrial forest inventories with different geographical scope (large-scale or small-scale) are carried out to collect quantitative data about forests. According to several authors (McRoberts and Tomppo, 2007; Nelson *et al.*, 2007; Koch and Dees, 2008), the utilization of remote sensing techniques can improve the efficiency and accuracy of forest inventories. Combining remote sensing data and field measurements facilitates the generation of detailed maps, showing the spatial distribution of forest attributes which cannot be achieved with *in situ* data alone.

One very important attribute measured during forest inventories is the height of trees. Height measurements are needed to determine the standing timber volume and are often used as an indicator to determine the production or growth potential of a site. The canopy height is well correlated with other forest attributes. Thus, height metrics derived from remote sensing data are usually the most useful variables to model, e.g. timber volume or biomass per hectare.

In this context, especially the potential of Light detection and ranging (LiDAR) technology was demonstrated in several research studies, e.g. carried out in boreal forests (Maltamo *et al.*, 2006; Næsset, 2007; Hyyppä *et al.*, 2008) or central European forests (Hollaus *et al.*, 2009; Latifi *et al.*, 2010; Breidenbach *et al.*, 2010). In some studies, the height information from LiDAR was combined with other remote sensing data for example medium-resolution satellite imagery (McInerney *et al.*, 2010).

Current innovations in the field of digital photogrammetry demonstrate the great potential of dense image matching algorithms for the derivation of high-resolution surface models (Haala, 2009; Leberl *et al.*, 2010; Hirschmüller, 2011). According to Leberl *et al.* (2010), dense image matching is defined as 'a match of multiple images at intervals as small as a pixel'. Dense matching based on aerial images was successfully applied to surface modelling in forests, e.g. using data acquired with digital frame cameras such as UltraCam X and XP (Straub and Seitz, 2011) or utilizing ADS 40 line scanner data (Waser *et al.*, 2011). If a LiDAR digital terrain

model (DTM) is available, to normalize the photogrammetric measurements, several variables related to the height and density of the vegetation can be derived and can be used as predictors to estimate further forest attributes, e.g. timber volume per hectare (Bohlin *et al*., 2012; Järnstedt *et al*., 2012; Straub *et al*., 2012).

Moreover, optical satellite-stereo imagery can be used to derive surface models for forests, and new satellites like WorldView-2 and GeoEye-1 allow more frequent and accurate stereo data acquisitions than before. A comprehensive overview of the characteristics and use of high-resolution optical satellite images is presented in Dowman *et al*. (2012). Compared with airborne remote sensing, satellite datasets have the following great advantages:

(1) High temporal resolution
(2) Great areal extent (large areas are covered by one satellite scene)

Some studies assessed the potential of optical satellite-stereo data to measure canopy heights. For example, Reinartz *et al*. (2005) used optical along track stereo imaging (SPOT-5 HRS) for forest height estimations in two different study sites, the first site located in the southeastern part of Bavaria and the second one in Catalonia, Spain. In St-Onge *et al*. (2008), the accuracy of forest height and biomass estimations were evaluated using an Ikonos stereo pair in combination with a LiDAR-DTM in a study site in Quebec, Canada. Wallerman *et al*. (2010) investigated 3D information derived from SPOT 5 stereo imagery and the airborne camera system Z/I DMC to map forest variables such as tree height, stem diameter and volume. Hobi and Ginzler (2012) analysed the height accuracy of surface models derived from WorldView-2 and ADS80 stereo data for different land cover types using GPS measurements, manual stereo-measurements and LiDAR data. Although the authors conclude that forests are the most challenging land cover types, high-resolution satellite stereo data were suggested as a valuable alternative to derive vegetation height information.

However, there is currently little experience of how accurate further forest attributes such as timber volume per hectare can be modelled using high-resolution ($\geq$1.0 m and $<$5 m) and very high-resolution ($<$1.0 m) satellite stereo data, particularly in heterogeneous forests with a complex vertical and horizontal structure. Thus, we assessed Cartosat-1 and WorldView-2 stereo imagery in combination with a LiDAR-DTM to estimate timber volume per hectare in a structurally rich forest area in Bavaria, Germany. All datasets were available for the same test site. The accuracies of both satellite datasets were evaluated both at plot and stand levels and were compared with estimations based on a LiDAR-Canopy height model (CHM). The potential and limitations of satellite stereo data for volume estimation within a small-scale forest inventory are demonstrated. Accuracies were evaluated for different forest structure types. Finally, advantages and disadvantages of satellite data for forest inventories are discussed.

Table 1 Tree species composition in Traunstein (as percentage of timber volume)

Tree Species	Percentage
Spruce (*Picea abies*)	49
Beech (*Fagus sylvatica*)	21
Fir (*Abies alba*)	15
Ash (*Fraxinus excelsior*)	5
Maple (*Acer pseudoplatanus*)	4
Other species	6

Materials and methods

Test site

A mixed and highly structured forest area close to the city of Traunstein in Bavaria, Germany, was selected as test site for this study (47°52′N 12°38′E). As shown in Table 1, the dominant tree species in the test site are spruce (*Picea abies* (*L*.) *H. Karsten*), beech (*Fagus sylvatica L*.) and fir (*Abies alba Mill*.). The forest stands in Traunstein represent a wide range of different age classes. Furthermore, the stands are mostly double- and multi-layered and have diverse densities as well as varying crown covers. The topography of the test site is characterized by an altitude range from 570 to 710 m with only a few steep slopes.

Remote sensing data

Three different remote sensing datasets were available for the test site:

(1) LiDAR data (separated into first and last echo points) were provided by the Bavarian Office for Surveying and Geographic Information (LVG, 2012). The LiDAR measurements were acquired at the end of March and beginning of April 2010 with a point density of 5–6 points m^{-2}. An automatic filtering algorithm, implemented in the software TreesVis (Weinacker *et al*., 2004a), was used to derive both a digital surface model (DSM) and a digital terrain model (DTM) with 1×1 m resolution. The filtering method is described in Elmqvist (2002) and Weinacker *et al*. (2004b).
(2) Cartosat-1 was launched on 5 May 2005 by the Indian Space Research Organization (ISRO). The sensor consists of two pushbroom cameras, which exhibit a forward view of $+26^{\circ}$ (Band F) and a nadir view of -5° (Band A). Each provides a 2.5 m spatial resolution panchromatic image with a swath width of 30 km and a maximum revisit time of 5 days (Satellite Imaging Corporation, 2012a). Three pairs of stereo data obtained in the year 2008 were used which were acquired on 25 February, 11 July and 3 November. As the Cartosat-1 stereo pairs were acquired at different acquisition dates, the leaf cover on deciduous trees was different. Dataset 1 was acquired at the end of February during leaf-off conditions, dataset 2 in July during leaf-on conditions and dataset 3 was acquired at the beginning of November partly during leaf-on conditions. Detailed acquisition parameters are shown in Table 2.
(3) WorldView-2 was launched on 8 October 2009. It provides 0.5 m panchromatic images and 2 m resolution 8 band multi-spectral images, four standard bands [red (0.630–0.690 μm), green (0.510–0.580 μm), blue (0.450–0.510 μm) and near-infrared 1 (0.770–0.895 μm)] and four new bands [coastal (0.400–0.450 μm), yellow (0.585–0.625 μm), red edge (0.705–0.745 μm) and near-infrared 2 (0.860–1.040 μm)]. WorldView-2 has a swath width of 16.4 km and a maximum revisit time of ~2 days (Satellite Imaging Corporation, 2012b). Stereo imagery, acquired on 19 June 2012 within one orbit through change of satellite pointing was used in this study (Table 3). As described in Table 3, stereo imagery with a small angle of convergence has been used.

Table 2 Acquisition parameters for Cartosat-1 images acquired for the Traunstein test site

	Dataset 1 (February)		Dataset 2 (July)		Dataset 3 (November)	
	Band A	Band F	Band A	Band F	Band A	Band F
Date, time (local)	25/02/2008, 10:04:30	25/02/2008, 10:03:38	11/07/2008, 10:07:08	11/07/2008, 10:06:16	03/11/2008, 10:07:25	03/11/2008, 10:06:32
Sensor azimuth (°)	194.7	14.2	194.7	14.1	194.7	14.1
Sensor elevation (°)	84.6	61.2	84.6	61.2	84.6	61.2
Sun azimuth (°)	157.6	157.4	146.12	145.7	167.8	167.6
Sun elevation (°)	30.4	30.3	60.8	60.7	26.1	26.1
Resolution (m)	2.5	2.5	2.5	2.5	2.5	2.5

Table 3 Acquisition parameters for WorldView-2 images acquired for the Traunstein test site

	First image	Second image
Date, time (local)	19/06/2012, 10:26:11	19/06/2012, 10:26:48
Sensor azimuth (°)	49.0	93.9
Sensor elevation (°)	62.6	73.0
Sun azimuth (°)	156.0	156.3
Sun elevation (°)	64.2	64.2
Resolution of panchromatic band (m)	0.5	0.5

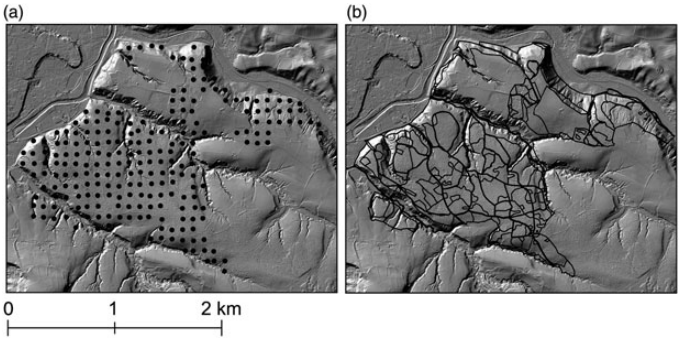

Figure 1 Relief image of Traunstein derived from a LiDAR-DTM with (a) location of forest inventory plots and (b) forest stand regions.

Field data

A forest inventory was carried out in Traunstein in summer 2008 by the staff of the Chair of Forest Yield Science of the Technical University of Munich. The standard inventory design of the Bavaria State Forest Enterprise was applied. A general description of the inventory design can be found in FER (2011). In total, 228 geo-referenced fixed area plots were distributed systematically over the entire forest area, using a 100×100 m grid, which are shown in Figure 1 a) superimposed on a shaded *relief image*. In addition, forest stand regions are visualized in Figure 1 b). The forest stands were delineated manually by a forest inventory specialist based on aerial photo interpretation supported by field surveys.

Due to the time difference between the field measurements and the acquisition of the remote sensing data, three plots were removed for the computations in this study because an obvious change in the forest structure was observed, e.g. as a result of timber harvesting or storm damage.

A Trimble GNSS receiver with a Zephyr Model 2 antenna was used to locate the field plot positions. Generally, the accuracy of these measurements had a maximum deviation of ± 3 m (R. Moshammer, personal communication, 16 May 2013).

Each sample plot consists of three concentric circles; the number of trees measured varied according to their diameter at breast height (DBH). Table 4 shows the radius and size of the different concentric circles and the DBH of trees to be measured within each circle. The largest circle with 500 m^2 was used as a reference region for the computations in this study. In addition to DBH measurements, tree heights were measured for some representative individuals at each plot. In multi-storied stands, heights were collected for all vertical layers.

During the inventory, each observed tree was assigned to one of the following vertical layers: (1) overstorey, (2) understorey, (3) regeneration and (4) emergent tree, whose crown emerges above the rest of the canopy. Based on this information, the plots were grouped into five forest structure types describing the vertical structure of the forest (Table 5).

Based on the single-tree measurements, timber volume V (m^3 ha^{-1}) was derived for each plot, defined as the usable volume of all trees in cubic metre under bark. The timber volume of the inventory plots in Traunstein has a great variation and ranges from 0 to 968 m^3 ha^{-1} with an arithmetic mean of 322 m^3 ha^{-1} and a standard deviation of 226 m^3 ha^{-1}.

Methods

Generation of surface and canopy height models using Cartosat-1 and WorldView-2 stereo imagery

The satellite DSMs used in this study were generated by semi-global matching (SGM), using census and mutual information as cost functions as described by Hirschmüller (2008) and d'Angelo *et al.* (2009). SGM based DSM generation is a powerful and robust method to achieve a high matching density and is also quick and easy to implement. The DSM generation procedure is described in detail in Tian *et al.* (2013). In satellite images, the radiometric information obtained can be very different when observing the forest from different viewing angles, and therefore, many areas might be presented as holes (match failed) in the directly obtained DSM. In order to improve the DSM quality, two different data fusion methods were considered for Cartosat-1 and WorldView-2 data respectively:

(1) Since more than one pair of stereo data were available for the Cartosat-1 data (within a short time period), all matched pixels from three pairs of stereo data were used to derive a DSM. Bundle block adjustment was performed beforehand to position the three pairs of stereo imagery in a consistent photogrammetric model in order to

Table 4 Concentric circles of sample plots with DBH of trees to be measured within each circle

Concentric Circle	Radius (m)	Size (m^2)	DBH (cm) of trees to be measured
1	3.15	31.15	≤9.9
2	6.31	125	10–29.9
3	12.62	500	≥30

Table 5 Classification of inventory plots into different forest structure types describing the vertical structure of the forest

No	Forest structure type	Acronym	Number of plots	Description
1	Single-layered	SL	26	Only trees with the attribute 'overstorey' occur at the sample plot and all trees have a height of >5 m
2	Double-layered	DL	114	Two combinations are possible: 1. trees with the attribute 'overstorey' and 'understorey' or 2. trees with the attribute 'overstorey' and 'regeneration' exist at the plot
3	Multi-layered	ML	44	Trees with the attributes 'overstorey', 'understorey' and 'regeneration' can be found at the plot
4	Juvenile	J	15	Only trees with the attribute 'overstorey' can be found at the plot and all trees have a height of ≤5 m
5	Emergent trees	ET	26	One or more trees with the attribute 'emergent tree' appear at the plot

have geometrically exactly the same location for pixels and height values. As Cartosat-1 can have bad direct georeferencing accuracy (shifts of >1 km were observed for some scenes), we used SRTM data as the reference during the bundle block adjustment (d'Angelo and Reinartz, 2012). Then, the three stereo-pairs were matched pairwise. Using this method, a denser and higher quality DSM with a resolution of 2.5 m and an absolute accuracy of ~ 5–10 m was generated.

(2) More than one band from WorldView-2 data were used to derive a DSM with 1 m resolution. For some land cover types (e.g. urban areas), high-resolution stereo imagery can provide clear features for matching, resulting in many successfully matched points and high-quality DSMs. However, in forest areas, high-resolution data sometimes can introduce noise. Moreover, forest areas are often more complex, since depending on the viewing direction, the sensor depicts different parts of the trees, which often represent different height values and which more often leads to matching failures. Therefore, an initial DSM (with 1 m resolution) generated from the high-resolution 0.5 m resolution panchromatic bands contained several holes (i.e. missing height values). To fill these holes, additional DSMs with 2 m resolution were generated using the green, near-infrared (NIR), in addition to the down-sampled panchromatic bands (the green and NIR bands were selected, due to their sensitivity to vegetation). To fill the missing height values, the additional DSMs were up-sampled to the initial DSM with 1 m resolution.

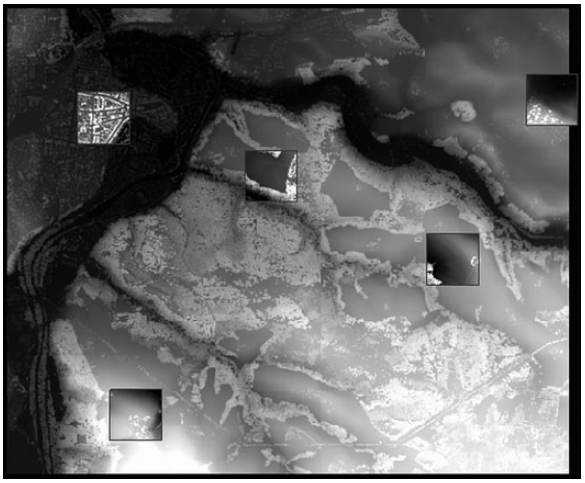

Figure 2 Selected regions used for 3D-shift determination.

An additional 3D co-registration was needed to remove any remaining overall displacement in all the three dimensions between the generated Cartosat-1 and WorldView-2 DSM and the LiDAR-DSM. As mentioned, an absolute accuracy of ~ 5–10 m was achieved for the Cartosat-1 data after the bundle block adjustment. For WorldView-2, the direct georeferencing accuracy is already in the range of 4.6–10.7 m (Satellite Imaging Corporation, 2012b). Therefore, small shifts of a few metres between all DSMs are expected. In order to improve the computation efficiency, we used a simple version of 3D least square matching, for which only the linear shifting is considered, the shift distances in three dimensions (X_s, Y_s, Z_s) are estimated via iterative 3D shift adjustment based on the minimization of:

$$\sum_{x=1}^{m}\sum_{y=1}^{n}\left(Z_{\text{ref}}(x,\,y)-(Z_{\text{2nd}}(x+X_s,\,y+Y_s)+Z_s)\right)^2 \qquad (1)$$

where m and n are the column and rows of the DSM, (x, y) are the planar coordinates and Z_{ref} and Z_{2nd} represent the height values from a reference DSM (LiDAR-DSM in this study) and the second DSM (DSM generated by stereo matching), respectively.

The shift-values X_s, Y_s and Z_s are iteratively adjusted to obtain a final shift result. In order to avoid unreasonable height differences (outliers) between two DSMs, a parameter was added to control the iterative procedure (referred to as 'outlier rate'). A percentage of very high height differences (e.g. possibly introduced by matching errors or changes) were defined as potential outliers (although probably only a portion of these height differences will be 'real' outliers, it is an easy and robust approach to get rid of extreme values). The percentage of height differences (which will not be used for the 3D co-registration) can be adjusted according to the DSM quality. In this study, we defined 0.5 per cent of the highest height differences as outliers, which can be used for most applications with Cartosat-1 and WorldView-2 data.

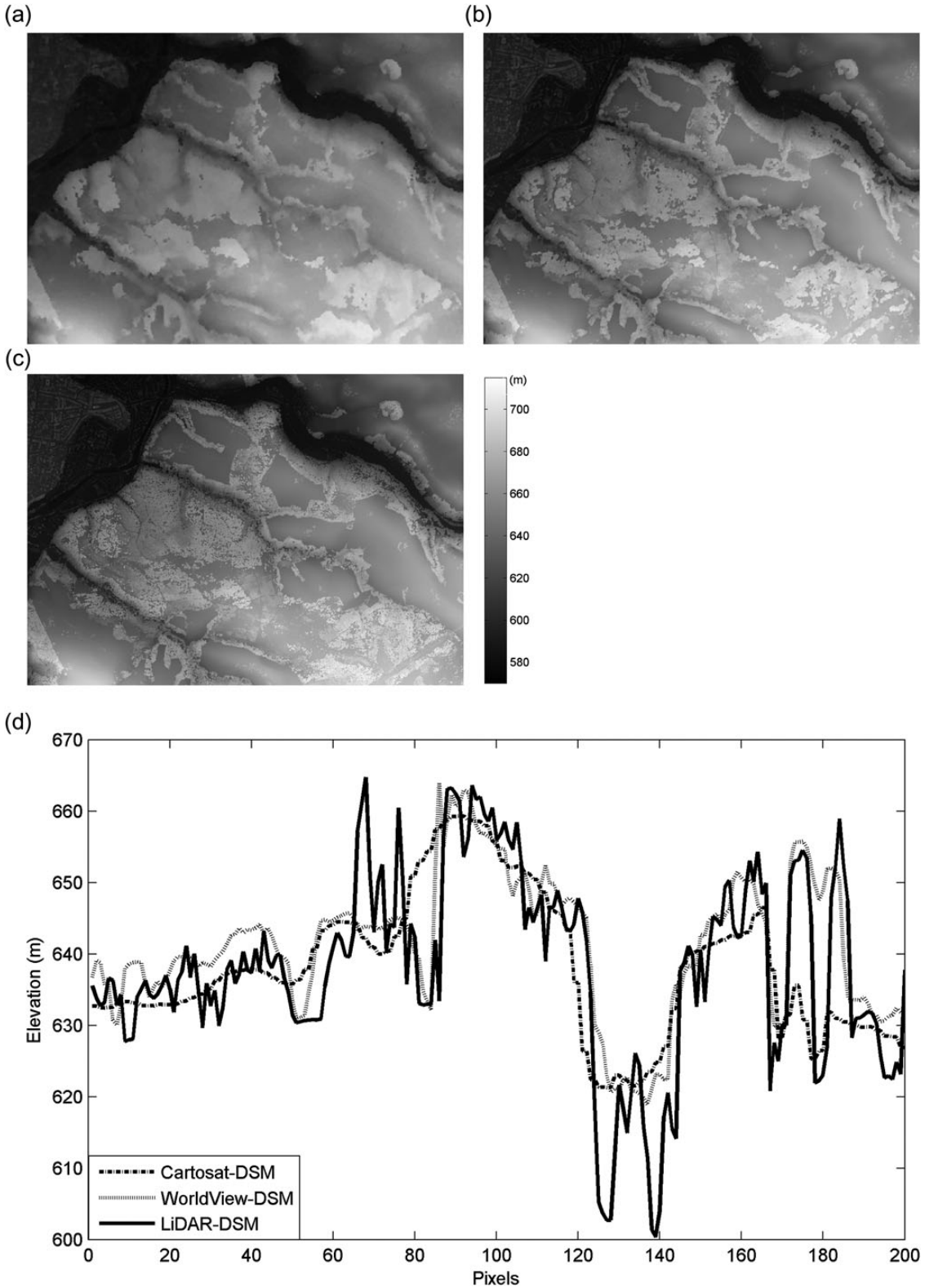

Figure 3 Grey value coded DSMs (a) Cartosat-1-DSM (a resolution of 2.5 m), (b) WorldView-2-DSM (1 m resolution) and (c) Lidar-DSM (1 m resolution) and (d) profile-comparison.

Since the study site is quite large and there might be variations in the forest areas, instead of using the whole DSMs, some regions, distributed consistently over the entire scene (Figure 2), which exhibit relatively flat terrain and low variation were chosen for the 3D co-registration. Then, the values from these regions were averaged to get a final shift value. Figure 3 shows the different surface models for Traunstein derived from Cartosat-1, WorldView-2 and LiDAR in addition to a comparison of profiles. In Figure 4, details of the DSMs are displayed as 3D views to show the amount of detail of the different surface models. Finally, CHMs were derived for all datasets by subtracting the LiDAR-DTM (for this purpose, the resolution of the LiDAR-DTM was adjusted to the corresponding resolution of the satellite DSMs, a resolution of 2.5 m for the Cartosat-1-DSM and 1 m resolution for the WorldView-2-DSM).

Estimation of timber volume at plot level

Ordinary least squares (OLS) regressions were used to quantify relations between remote sensing variables and field measurements at forest inventory plots in Traunstein. A linear model (which was also applied in other studies, e.g. Tonolli *et al.*, 2011 or Straub and Koch, 2011) was used to predict timber volume:

$$V = \beta_0 + \beta_1 X_1 + \beta_2 X_2 + \cdots + \beta_n X_n + \varepsilon \quad (2)$$

where V = timber volume (m^3 ha^{-1}), X_i = independent variables (derived from CHMs) $i = 1, \ldots, n$, β_i = regression coefficients $i = 0, \ldots, n$, ε = error term.

For all remote sensing datasets (Cartosat-1, WorldView-2 and LiDAR), the same explanatory variables were derived from the CHMs separately for each inventory plot:

1. Height metrics: minimum height h_{min}, first quartile h_{25}, median h_{50}, arithmetic mean h_m, third quartile h_{75} and maximum height h_{max}
2. The canopy cover (*cc*) was estimated as a measure for the density of the forest. Crown regions were extracted using a height threshold of 2 m (as suggested by Nilsson, 1996; Næsset, 2002; Maltamo *et al.*, 2006) to estimate the percentage of crown areas covering the forest floor.
3. The surface roughness (sr) was quantified by fitting a plane to the height values at each inventory plot. The coefficients of the plane were estimated through least squares adjustment using the height values of the CHM as reference points. The surface roughness was computed based on the vertical height deviations between the height values of the CHM and the plane:

$$sr = \sqrt{\frac{1}{n}\sum_{i=1}^{n}(h_i - \hat{h}_i)^2} \quad (3)$$

where h_i = height value of point i on the CHM, $\hat{h}_i$ = height value of point i on the plane, n = number of height values within the inventory plot.

All the 225 inventory plots were used for the regressions. First, a stepwise variable selection was applied to automatically select significant variables. The goodness-of-fit of the models was determined by the multiple coefficient of determination (R^2) and adjusted R^2 (Adj. R^2), which is a modification of the R^2 that adjusts for the number of predictors in the model (Dowdy *et al.*, 2004). To evaluate the prediction accuracy of the models, the absolute and relative root mean squared errors (RMSEs) and bias were computed using leave-one-out cross-validation.

In addition to a linear relationship, also non-linear relationships were tested to predict timber volume, using logarithmic transformations of the variables for the regression as, for example, described in Means *et al.* (2000); Næsset (2002) or Hollaus *et al.* (2007). Finally, the linear relationship (without transformations) was selected to predict timber volume in this study, as it performed best with respect to the cross-validated RMSEs and with respect to scatterplots of predicted versus observed timber volume.

Estimation of timber volume at stand level

A practical two-phase procedure as suggested by Næsset (2002) was used to derive volume estimations for the entire forest area. In the first phase, regressions were used to identify relations between remote sensing metrics and field measurements at plot level (as described in section Estimation of timber volume at plot level). In the second phase, the regression models were used to estimate a forest attribute for the entire forest area by subdividing the forest into cells, each with the same size as an inventory plot. Then, estimations for individual forest stands can be derived by intersecting the cells with stand regions.

To assess the accuracy of the volume estimation at stand level, a validation method as described in Bohlin *et al.* (2012) was applied [which Bohlin *et al.* (2012) named 'leave-one-stand-out cross-validation']. As described above, the test site was subdivided into cells, each with the same size as an inventory plot (here: 500 m^2). Within each cell, all necessary explanatory variables were derived separately for each remote sensing dataset. To estimate timber volume per hectare for cells within a specific stand, all

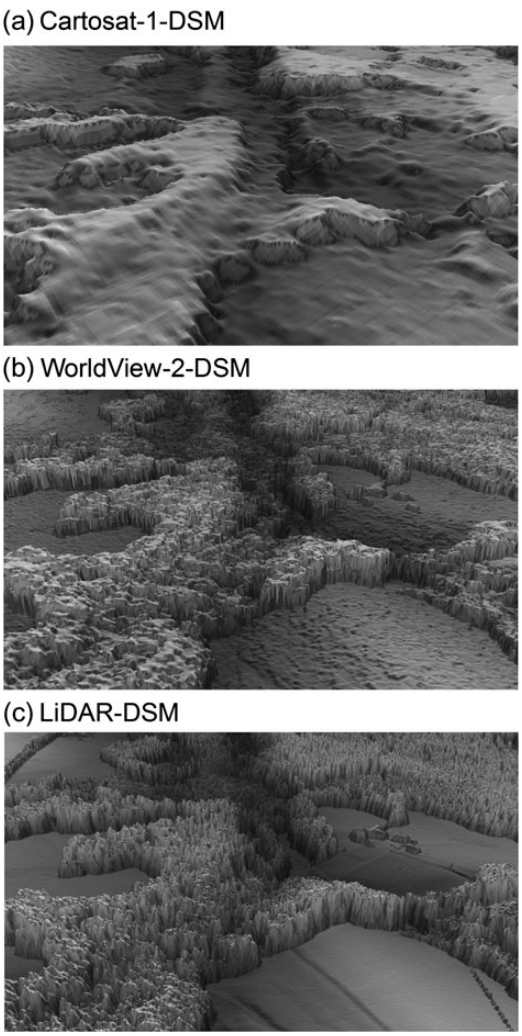

Figure 4 3D view of (a) Cartosat-1-DSM (2.5 m resolution), (b) WorldView-2-DSM (1 m resolution) and (c) LiDAR-DSM (1 m resolution).

inventory plots located within the stand region were defined as test set. Only plots outside of the stand region were used as training set to derive the regression coefficients. After estimating timber volume for each cell separately, the cells were intersected with the stand polygons and the stand volume was predicted as area-weighted average of the cell estimates (thus, truncated cells at the stand border obtained a lower weight). Finally, the predicted stand volume was compared with the average of the timber volume of field plots located within each stand region (the test set), using absolute and relative RMSE and bias (Table 6).

Following Bohlin *et al.* (2012), only stands with at least 6 inventory plots were used for the validation, which resulted in 13 validation stands in Traunstein with an average stand size of 10 ha. The stand volume of the validation stands ranges from 43 $m^3\ ha^{-1}$ to 595 $m^3\ ha^{-1}$ with an arithmetic mean of 334 $m^3\ ha^{-1}$ and a standard deviation of 181 $m^3\ ha^{-1}$.

Results

Table 7 shows the different OLS regression models generated using Cartosat-1, WorldView-2 or LiDAR data to estimate the timber volume per hectare V ($m^3\ ha^{-1}$). The variables are listed according to their importance to estimate V. In addition to unstandardized regression coefficients, also standardized coefficients are listed, to show the relative importance of the predictors. For both satellite datasets (Cartosat-1 and WorldView-2), it was possible to develop suitable models for timber volume estimation. The scatter of volume estimations at plot level is quite similar for the satellite datasets and the LiDAR data (as shown in Figure 5). In all cases, the scatter increases with increasing timber volume. In addition, the boxplots in Figure 6 illustrate that the error distribution (within different forest structure types) is comparable for all datasets. As expected, the errors for volume estimation are higher for double and multi-layered plots, compared with single layered plots, which can be explained by the fact that only the overstorey can be captured in the surface models. Nevertheless, trees in the overstorey contribute most to the timber volume. The scatterplots in Figure 7 demonstrate that the scatter was reduced considerably when the estimation at plot level was aggregated to the stand level for evaluation.

Table 6 Absolute and relative RMSE and bias for the timber volume estimation at stand level

Dataset	RMSE ($m^3\ ha^{-1}$)	RMSE (%)	Bias ($m^3\ ha^{-1}$)	Bias (%)
Cartosat-1	71.84	21.49	9.11	2.73
WorldView-2	65.49	19.59	5.77	1.73
LiDAR	57.30	17.14	9.49	2.84

Discussion and outlook

In this study, high-resolution canopy surface models were successfully derived from both Cartosat-1 and WorldView-2 stereo data using SGM. In general, recognizable textures in the images are a precondition for an image-matching algorithm. In a forest area, the following factors may influence the success of an image-matching procedure to find corresponding image points:

(1) Vertical forest structure: As shown in Figure 8, in forests with high surface roughness, the nadir views may see different parts of the tree crowns compared with the forward views, and partly may lead to wrong matching results.
(2) Due to the different viewing direction of the stereo pair and the angle between sun illumination and object orientation, the reflection of the tree surface may be quite different (BRDF-effect for a forest canopy). Additionally, the two views exhibit about half to one minute time difference. Within this time interval, the trees can have different reflectance characteristics, e.g. due to wind. Thus the stereoscopic images may see different parts of the leaves and crowns.
(3) Illumination: Depending on the topography and sun angle, DSM quality is generally worse in shadow areas and near the forest boundary. The difficulty of occlusion and shading for image matching in forests was also described by Korpela and Anttila (2004).
(4) Additionally, the season will also influence DSM quality, since during leaf-off conditions (for deciduous trees) the matching partly does not extract the canopy but the ground. However, still more research is needed to analyse satellite images acquired for different phenological stages, e.g. to investigate

Table 7 OLS regression models to estimate timber volume V ($m^3\ ha^{-1}$) based on Cartosat-1, WorldView-2 and LiDAR metrics (RMSEs and bias for the estimation at plot level are specified)

Data source	Variable	Coefficients		R^2	Adj. R^2	RMSE ($m^3\ ha^{-1}$)	RMSE (%)	Bias ($m^3\ ha^{-1}$)	Bias (%)
		Unstandardized	Standardized						
Cartosat-1	h_m	16.487	0.701	0.492	0.489	161.819	50.26	−0.04	0.01
	Intercept	31.854							
WorldView-2	h_{75}	11.042	0.469	0.615	0.608	142.967	44.40	0.16	0.05
	h_{25}	9.848	0.423						
	cc	−1.435	−0.137						
	sr	15.693	0.150						
	Intercept	25.691							
LiDAR	h_m	24.968	0.965	0.710	0.708	122.437	38.02	0.02	0.01
	cc	−1.430	−0.165						
	Intercept	−0.432							

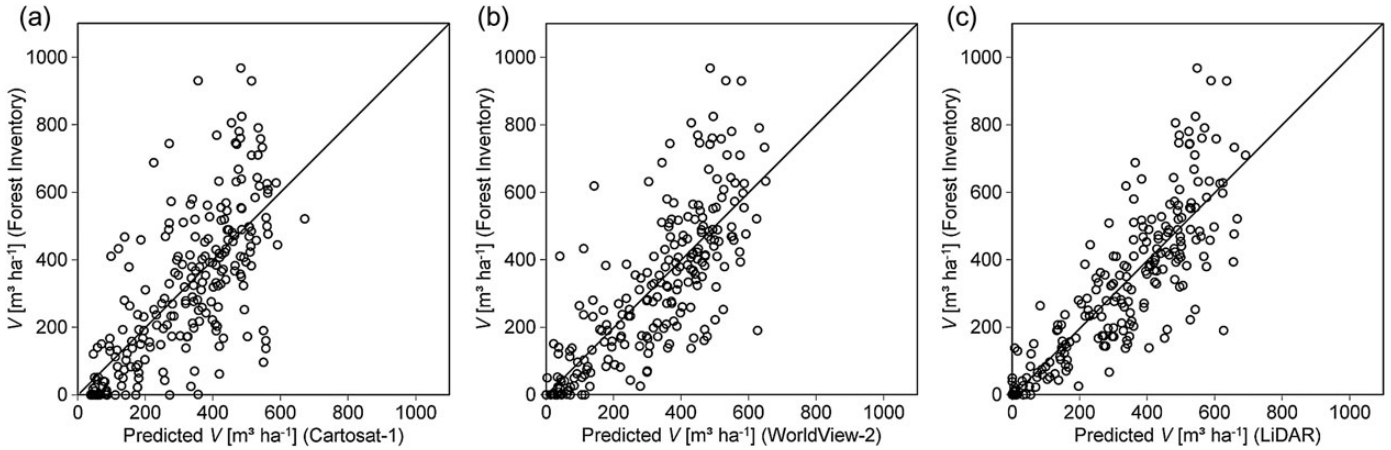

Figure 5 Predicted V (m^3 ha^{-1}) for inventory plots plotted against the observed timber volume of the forest inventory based on (a) Cartosat-1 (b) WorldView-2 and (c) LiDAR.

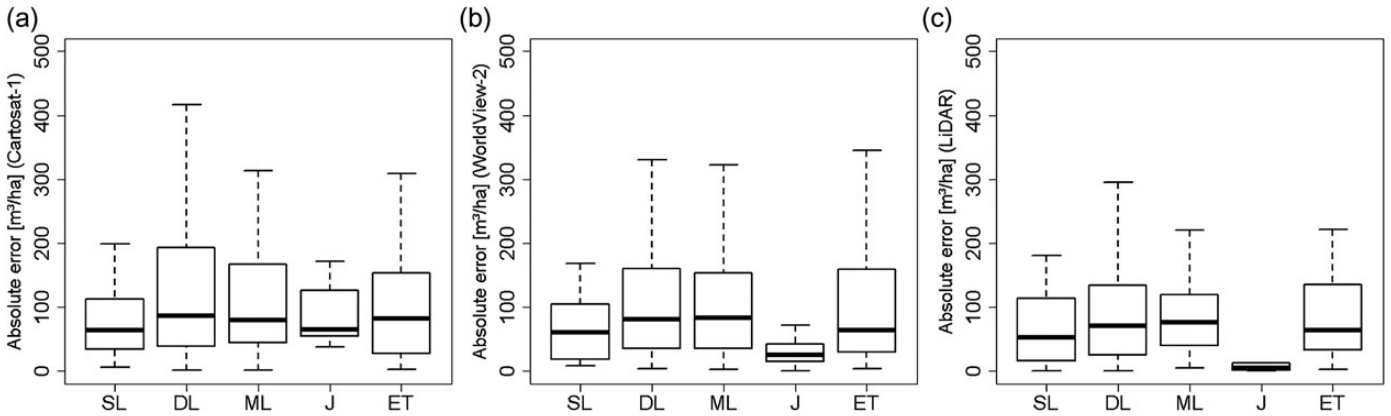

Figure 6 Boxplots of absolute errors for the estimation of V (m^3 ha^{-1}) at plot level in different vertical forest structure types (as defined in Table 5), using (a) Cartosat-1, (b) WorldView-2 and (c) LiDAR (the plot whiskers extend to 1.5 × interquartile range from the box).

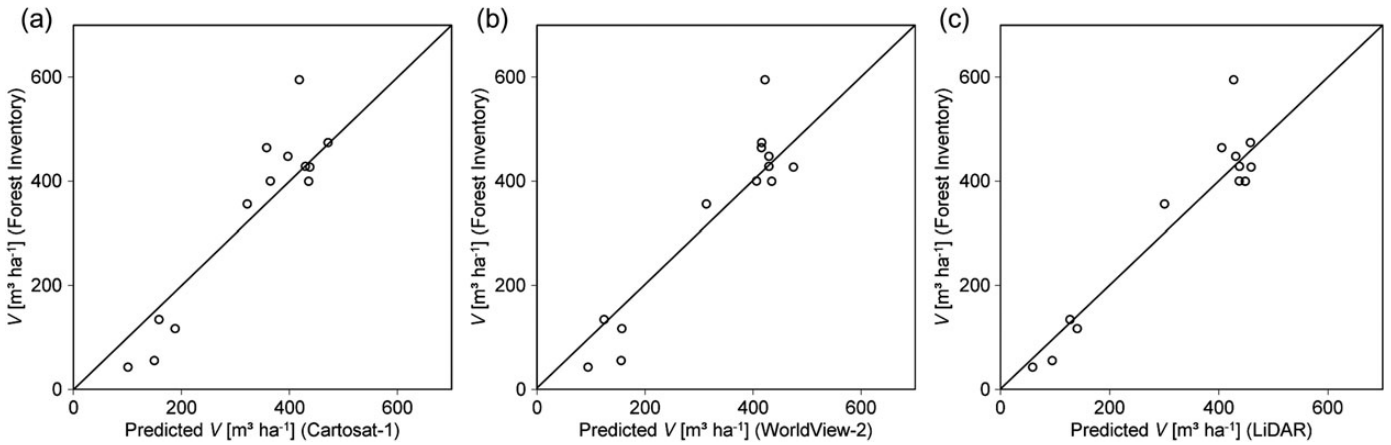

Figure 7 Predicted V (m^3 ha^{-1}) for 13 validation stands plotted against the mean timber volume of inventory plots located within the stand regions for (a) Cartosat-1 (b) WorldView-2 and (c) LiDAR.

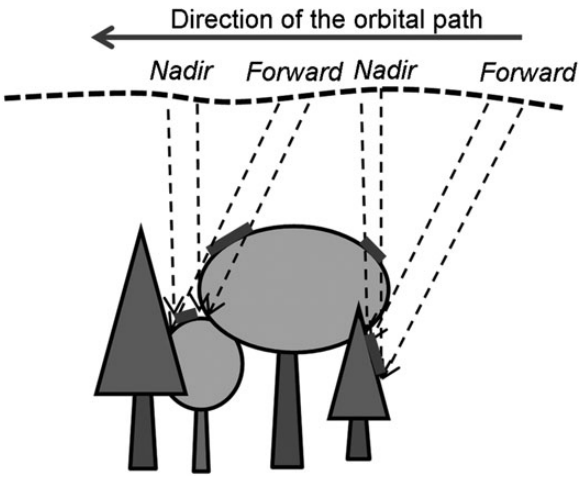

Figure 8 Nadir views compared with forward views in forests with high surface roughness.

the effect of leaf-off conditions on the quality of DSMs for different forest types with different species and with different species mixture.

Visual assessment revealed that most serious differences between the satellite DSMs and the LiDAR-DSM occurred in very sparse forest stands with just a few scattered single trees or small groups of trees, which often cannot be detected in the canopy surfaces resulting from satellite data. However, for forest stands with closed canopies and low height variation of the trees, estimated stand heights were very similar to those in the LiDAR-DSM.

The comparison with a LiDAR-CHM demonstrated that timber volume can be predicted with fair accuracy based on Cartosat-1 and with very satisfying accuracy using WorldView-2 data (at plot level). In both cases the RMSEs for timber volume estimation were smaller than the standard deviation of the observed timber volume. As a very complex test site was selected for this study (with a great species mixture, many different age classes and many multi-layered stands), we expect even lower errors in more homogeneous forests.

Although the time difference to the field measurements is much higher for the WorldView-2 data (compared with Cartosat-1 data), the RMSE at plot level is considerably lower for WorldView-2, which shows that the estimation accuracy depends a lot on the spatial resolution (1 m and 2.5 m) and thus the level of detail of the surface models derived from the remote sensing data in the present case.

As expected, height metrics are the most important predictors for timber volume estimation. Nevertheless, in case of WorldView-2 and LiDAR, the canopy cover *cc* was selected as an additional contributing variable for volume estimation. In the case of Cartosat-1 *cc* did not improve the estimation significantly, which might be due to the fact that the resolution of the Cartosat-1 model is too low to characterize the percentage of crown areas covering the forest floor accurately enough.

The scatterplots in Figure 5 indicate saturation for relatively high timber volume values (at $\sim 600\ m^3\ ha^{-1}$), especially for Cartosat-1. Nevertheless, just a few field plots exceed $600\ m^3\ ha^{-1}$ in Traunstein. Thus, in future studies, timber volume estimation should be tested in other mixed European forests with even larger growing stocks.

Moreover, a positive systematic error (bias) was observed at stand level which is very similar for both the satellite and the LiDAR data sets; the bias, however, is very low (ranging from 1.73 to 2.84 per cent).

In conclusion, the results of this experimental study have demonstrated the potential of WorldView-2 and Cartosat-1 stereo data for a regionalization of sample plot inventories to generate maps, showing the spatial distribution of timber volume at stand level which frequently cannot be achieved with *in situ* data alone. The LiDAR technology is generally considered the most accurate remote sensing technique for estimating forest attributes such as timber volume (Järnstedt *et al.* 2012). Thus, a LiDAR-DSM was used as reference in this study. However, it is widely recognized that LiDAR surveys are considerably more expensive than satellite data acquisition (McInerney *et al.*, 2010). Still, a LiDAR-DTM is required to derive canopy height information from the satellite DSMs. These LiDAR–DTMs are often available in European countries from LiDAR campaigns carried out by the national or regional mapping agencies, e.g. such a DTM exists for the entire state of Bavaria in Germany. Hence, as suggested by St-Onge *et al.* (2008), surface models derived from stereo satellite data used in combination with an existing LiDAR-DTM can be an economical alternative to LiDAR surveys to derive CHMs and to estimate timber volume, especially for large regions. Another major advantage of satellite data is the high temporal resolution. Terrestrial forest inventories in Germany are typically updated every 10 years. Satellite data can enable much more frequent data acquisition, which may be particularly suitable for change detection analysis, e.g. to obtain rapid information about changes in the forest structure, e.g. due to timber harvest, storm or other biotic or abiotic factors.

In this study, satellite CHMs were co-registered with field plots from a small-scale forest inventory. As large areas can be covered by one satellite scene ($225\ km^2$ for Worldview-2 and $900\ km^2$ for Cartosat-1), satellite-derived surface models possibly will be suitable for integration into large-scale forest inventories. Thus, in a future project, it is intended to estimate timber volume for much larger regions using field plots from the German National Forest Inventory (NFI) where the sample distribution is based on a nationwide 4×4 km quadrangle grid (BMELV, 2012). In future, we also intend to estimate further forest attributes such as basal area per hectare or mean stem diameter.

Acknowledgements

The authors thank Dr. P. d'Angelo for providing his support in DSM generation. They also express their gratitude to the Chair of Forest Yield Science of the Technische Universität München for providing the field data for this research study and European Space Imaging (EUSI) and euromap GmbH for providing WorldView-2 and Cartosat-1 stereo data, respectively, for scientific purposes.

Funding

This research was funded by the Bavarian State Ministry of Food, Agriculture and Forestry.

References

BMELV 2012 *The National Forest Inventory – NFI (Bundeswaldinventur)*. Federal Ministry of Consumer Protection, Food and Agriculture (Bundesministerium für Ernährung, Landwirtschaft und Verbraucherschutz), http://www.bundeswaldinventur.de/enid/a9.html (accessed on 11 December, 2012).

Bohlin, J., Wallerman, J. and Fransson, J.E.S. 2012 Forest variable estimation using photogrammetric matching of digital aerial images in combination with a high-resolution DEM. *Scan. J. For. Res.* **27**, 692–699.

Breidenbach, J., Nothdurft, A. and Kändler, G. 2010 Comparison of nearest neighbour approaches for small area estimation of tree species-specific forest inventory attributes in central Europe using airborne laser scanner data. *Eur. J. For. Res.* **129**(5), 833–846.

d'Angelo, P. and Reinartz, P. 2012 DSM based orientation of large stereo satellite image blocks. *Int. Arch. Photogramm. Remote Sens. Spatial Inf. Sci.* **39**(B1), 209–214.

d'Angelo, P., Schwind, P., Krauss, T., Barner, F. and Reinartz, P. 2009 Automated DSM based georeferencing of Cartosat-1 stereo scenes. *Int. Arch. Photogramm. Remote Sens. Spatial Inf. Sci.* **38-1-4-7/W5**, 1–6.

Dowdy, S., Wearden, S. and Chilko, D. 2004 *Statistics for research*. 3rd edn. Wiley series in probability and statistics, Wiley, 627 pp.

Dowman, I., Jacobsen, K., Konecny, G. and Sandau, R. 2012 *High resolution optical satellite imagery*. Whittles Publishing, Scotland, UK, 230 pp.

Elmqvist, M. 2002 Ground surface estimation from airborne laser scanner data using active shape models. *Int. Arch. Photogramm. Remote Sens. Spatial Inf. Sci.* **34**(3A), 114–118.

FER 2011 *Richtlinie für die mittel- und langfristige Forstbetriebsplanung in den Bayerischen Staatsforsten. Forsteinrichtungsrichtlinie – FER 2011*. Bayerische Staatsforsten (Bavaria State Forest Enterprise), Regensburg.

Haala, N. 2009 Comeback of digital image matching. In *Photogrammetric Week 09*. Fritsch, D. (ed). Wichmann, Heidelberg, pp. 289–301.

Hirschmüller, H. 2008 Stereo processing by semiglobal matching and mutual information. *IEEE Trans. Pattern Anal. Mach. Intell.* **30**(2), 1–14.

Hirschmüller, H. 2011 Semi-Global Matching – motivation, developments and applications. In *Photogrammetric Week 11*. Fritsch, D. (ed). Wichmann, Heidelberg, pp. 173–184.

Hobi, M.L. and Ginzler, C. 2012 Accuracy assessment of digital surface models based on WorldView-2 and ADS80 stereo remote sensing data. *Sensors* **12**(5), 6347–6368.

Hollaus, M., Wagner, W., Maier, B. and Schadauer, K. 2007 Airborne laser scanning of forest stem volume in a mountainous environment. *Sensors* **7**, 1559–1577.

Hollaus, M., Wagner, W., Schadauer, K., Maier, B. and Gabler, K. 2009 Growing stock estimation for alpine forests in Austria: a robust lidar-based approach. *Can. J. For. Res.* **39**(7), 1387–1400.

Hyyppä, J., Hyyppä, H., Leckie, D.G., Gougeon, F.A., Yu, X. and Maltamo, M. 2008 Review of methods of small-footprint airborne laser scanning for extracting forest inventory data in boreal forests. *Int. J. Remote Sens.* **29**(5), 1339–1366.

Järnstedt, J., Pekkarinen, A., Tuominen, S., Ginzler, C., Holopainen, M. and Viitala, R. 2012 Forest variable estimation using a high-resolution digital surface model. *ISPRS J. Photogramm.* **74**, 78–84.

Koch, B. and Dees, M. 2008 Forestry applications. In *Advances in Photogrammetry, Remote Sensing and Spatial Information Sciences*. Li, Z., Chen, J. and Baltsavias, E. (eds). Taylor and Francis Group, London, pp. 439–465.

Korpela, I. and Anttila, P. 2004 Appraisal of the mean height of trees by means of image matching of digitised aerial photographs. *Photogramm. J. Finland* **19**(1), 23–36.

Latifi, H., Nothdurft, A. and Koch, B. 2010 Non-parametric prediction and mapping of standing timber volume and biomass in a temperate forest: application of multiple optical/LiDAR-derived predictors. *Forestry* **83**(4), 395–407.

Leberl, F., Irschara, A., Pock, T., Meixner, P., Gruber, M. and Scholz, S *et al*. 2010 Point clouds: Lidar versus 3D vision. *Photogramm. Eng. Remote Sens.* **76**(10), 1123–1134.

LVG 2012 *Digitale Geländemodelle (DGM). Product information of the Bavarian Office for Surveying and Geographic Information (Landesamt für Vermessung und Geoinformation Bayern)* http://vermessung.bayern.de/file/pdf/1614/download_faltblatt-dgm09.pdf (accessed on 11 December, 2012).

Maltamo, M., Malinen, J., Packalén, P., Suvanto, A. and Kangas, A. 2006 Nonparametric estimation of stem volume using airborne laser scanning, aerial photography and stand-register data. *Can. J. For. Res.* **36**(2), 426–436.

McInerney, D.O., Suarez-Minguez, J., Valbuena, R. and Nieuwenhuis, M. 2010 Forest canopy height retrieval using LiDAR data, medium-resolution satellite imagery and *k*NN estimation in Aberfoyle, Scotland. *Forestry* **83**(2), 195–206.

McRoberts, R.E. and Tomppo, E.O. 2007 Remote sensing support for national forest inventories. *Remote Sens. Environ.* **110**, 412–419.

Means, J.E., Acker, S.A., Fitt, B.J., Renslow, M., Emerson, L. and Hendrix, C.J. 2000 Predicting forest stand characteristics with airborne laser scanning LIDAR. *Photogramm. Eng. Remote Sens.* **66**(11), 1367–1371.

Næsset, E. 2002 Predicting forest stand characteristics with airborne scanning laser using a practical two-stage procedure and field data. *Remote Sens. Environ.* **80**(1), 88–99.

Næsset, E. 2007 Airborne laser scanning as a method in operational forest inventory: status of accuracy assessments accomplished in Scandinavia. *Scan. J. For. Res.* **22**(5), 433–422.

Nelson, M., Moisen, G., Finco, M. and Brewer, K. 2007 Forest inventory and analysis in the united states: remote sensing and geospatial activities. *Photogramm. Eng. Remote Sens.* **73**(7), 729–732.

Nilsson, M. 1996 Estimation of tree heights and stand volume using an airborne lidar system. *Remote Sens. Environ.* **55**, 1–7.

Reinartz, P., Müller, R., Hoja, D., Lehner, M. and Schroeder, M. 2005 *Comparison and fusion of DEM derived from SPOT-5 HRS and SRTM data and estimation of forest heights*. Earsel Workshop 3D-Remote Sensing, Earsel Symposium, Porto, Portugal.

Satellite Imaging Corporation 2012a Cartosat-1 Satellite Sensor. http://www.satimagingcorp.com/satellite-sensors/cartosat-1.html (accessed on 26 November, 2012).

Satellite Imaging Corporation 2012b WorldView-2 Satellite Sensor. http://www.satimagingcorp.com/satellite-sensors/worldview-2.html (accessed on 26 November, 2012).

St-Onge, B., Hu, Y. and Vega, C. 2008 Mapping the height and above-ground biomass of a mixed forest using lidar and stereo Ikonos images. *Int. J. Remote Sens.* **29**(5), 1277–1294.

Straub, C. and Koch, B. 2011 Enhancement of bioenergy estimations within forests using airborne laser scanning and multispectral line scanner data. *Biomass and Bioenergy* **35**(8), 3561–3574.

Straub, C. and Seitz, R. 2011 Möglichkeiten der automatisierten Generierung von Oberflächenmodellen in Waldgebieten aus digitalen Luftbildern. In *Proceedings of the 31st Annual Meeting of the DGPF (German Society for Photogrammetry and Remote Sensing)*. Seyfert, E. (ed). Publication of the DGPF, Potsdam, pp. 153–162.

Straub, C., Seitz, R. and Waser, L.T. 2012 Comparison of digital aerial images and airborne laser scanning data for timber volume estimation on plot level. *ForestSAT 2012 conference*, 11-14 September, Oregon State University, Corvallis, OR, USA.

Tian, J., Reinartz, P., d'Angelo, P. and Ehlers, M. 2013 Region-based automatic building and forest change detection on Cartosat-1 stereo imagery. *ISPRS J. Photogramm. Remote Sens.* **79**, 226–239.

Tonolli, S., Dalponte, M., Vescovo, L., Rodeghiero, M., Bruzzone, L. and Gianelle, D. 2011 Mapping and modelling forest tree volume using forest inventory and airborne laser scanning. *Eur. J. For. Res.* **130**(4), 569–577.

Wallerman, J., Fransson, J.E.S., Bohlin, J., Reese, H. and Olsson, H. 2010 Forest mapping using 3D data from SPOT-5 HRS and Z/I DMC. In *Proceedings of the IEEE International Geoscience & Remote Sensing Symposium (IGARSS)*, 25–30 July, Honolulu, Hawaii, USA, pp. 64–67.

Waser, L.T., Ginzler, C., Kuechler, M., Baltsavias, E. and Hurni, L. 2011 Semi-automatic classification of tree species in different forest ecosystems by spectral and geometric variables derived from Airborne Digital Sensor (ADS40) and RC30 data. *Remote Sens. Environ.* **115**(1), 76–85.

Weinacker, H., Koch, B. and Weinacker, R. 2004a TREESVIS – a software system for simultaneous 3D real-time visualization of DTM, DSM, laser raw data, multispectral data, simple tree and building models. *Int. Arch. Photogramm. Remote Sens. Spatial Inf. Sci.* **36**(8/W2), 90–95.

Weinacker, H., Koch, B., Heyder, U. and Weinacker, R. 2004b Development of filtering, segmentation and modelling modules for LIDAR and multispectral data as a fundamental of an automatic forest inventory system. *Int. Arch. Photogramm. Remote Sens. Spatial Inf. Sci.* **36**(8/W2), 50–55.